

- [29] M. A. van Dijk, R. van den Berg, *Macromolecules* **1995**, *28*, 6773.
 [30] From the morphology of the polymer blend thin film, it was already pointed out that there is no clear affinity for one of the two hydrophobic phases to preferentially wet the hydrophilic silicon substrate.
 [31] V. Z.-H. Chan, E. L. Thomas, R. G. H. Lammertink, M. A. Hempenius, G. J. Vancso, H. Wang, R. J. Composto, unpublished.
 [32] Auger electron spectroscopy (AES) data obtained for oxygen etched PFS homopolymer are consistent with the XPS results. Depth profiling (argon ion sputtering) indicated an approximately 10 nm thin layer rich of iron, silicon, and oxide at the surface of the oxygen etched polymer film.
 [33] A. B. Fischer, J. B. Kinney, R. H. Staley, M. S. Wrighton, *J. Am. Chem. Soc.* **1979**, *101*, 6501.

Formation of Mesoporous Silica Nanotubes**

By Hong-Ping Lin, Chung-Yuan Mou,*
and Shang-Bin Liu

Since the discovery of M41S mesoporous materials,^[1,2] considerable efforts have been made to modify its structural features; pore size (in a few nanometers) and morphology (in micron or millimeter scale) being two of the most studied examples. Control over both parameters would have a crucial impact on understanding of biomineralization, and would extend the potential applications of these mesoporous materials. The control of the order in the above scales is usually studied as two independent problems. Now through a special post-synthesis-ammonia hydrothermal treatment, we are able however to simultaneously re-structure pore size, nano-channel regularity and morphology of the mesoporous materials prepared from acid route. The re-structured products become highly ordered and more stable while giving nano-sized tubular form of the silica. Mesoporous silica tubes of diameter around 30–100 nm were formed. This is the smallest tubular form observed in mesoporous silica. In such process, we also find that a novel topological transformation takes place in gyroidal spheres.

We have previously employed the acidic route invented by Huo et al.^[3] to manufacture silica ropes^[4] and gyroidal spheres.^[5] The silica ropes (from C₁₈TMAB (TMAB = trimethylammonium bromide)) and gyroids (from C₁₆TMAB) were successfully prepared in high yields, (>90%). Although the morphology was preserved after calcination, the hexagonal structure became less ordered and a large *d*₁₀₀-spacing shrinkage of about 0.3–0.6 nm.

We thus considered the effect of post-synthesis-ammonia hydrothermal treatments on these two samples. After ammonia hydrothermal treatment at 150 °C for 2 days, the two

products exhibit 5 to 7 sharp XRD peaks (Fig. 1A,B) while the products before hydrothermal treatment only have 2 to 4 broader peaks (Fig. 1C,D). The existence of the higher order reflection peaks (Fig 1A, 1B) such as 300, 220, and 310, suggests that well-aligned MCM-41 structures are formed. There is also a lattice expansion of the *d*-spacings by 1.4 and 1.3 nm after the hydrothermal re-structuring.^[6–8] The shrinkage of the *d*₁₀₀ value, after calcination, of these treated samples is only 0.1 nm. From the ²⁹Si magic angle spinning nuclear magnetic resonance (MASNMR) spectra of the as-synthesized materials before and after ammonia hydrothermal treatment, the Q₃ (Si(OSi)₃OH)/Q₄ (Si(OSi)₄) ratio changes from 1.0 to 0.4. This indicates that the silica structure further condenses during ammonia hydrothermal treatment and makes it more thermally stable.

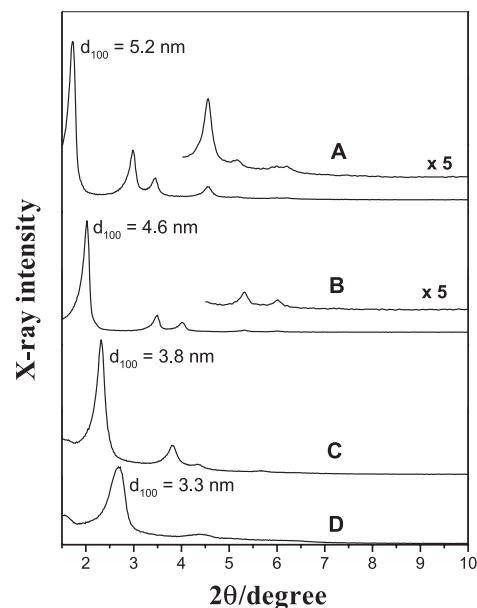


Fig. 1. XRD patterns of the calcined materials obtained from C_nTMAX–HNO₃–TEOS–H₂O systems with (A,B) and without (C,D) hydrothermal treatment: A) C₁₈TMACl; B) C₁₆TMAB; C) C₁₈TMAB; D) C₁₆TMAB.

Figure 2 shows the N₂ adsorption–desorption isotherms of the mesoporous materials before and after ammonia hydrothermal treatment at various times and temperatures. The sample without hydrothermal treatment has broader pore size distribution (full width at half maximum, FWHM = 1.2 nm; Fig. 2A). This is because the meso-structure is inherently unstable and some structural collapse occurs during calcination. After ammonia hydrothermal treatment, the samples possess a sharp pore-size distribution of FWHM about 0.1–0.18 nm (Fig. 2B–D). Notably, increasing the hydrothermal time and temperature to 150 °C can expand the pore size to about 5.0 nm.

These results show that the ammonia hydrothermal process would not only re-structure the nano-structure of the silica ropes and gyroidal spheres under acidic conditions into a highly ordered nano-structure, but would also increase the thermal and hydrothermal stability of the nano-structure.

[*] Dr. C.-Y. Mou
Department of Chemistry, National Taiwan University
Taipei, 106 (Taiwan)

Dr. H.-P. Lin, Dr. S.-B. Liu
Institute of Atomic and Molecular Sciences Academia Sinica
P. O. Box 23-166, Taipei, 106 (Taiwan)

[**] We thank Chih-Yuan Tang for help in TEM and SEM microscopy. This research was supported by the China Petroleum Co. and the National Science Council of Taiwan (NSC 88-2113-M-002-027).

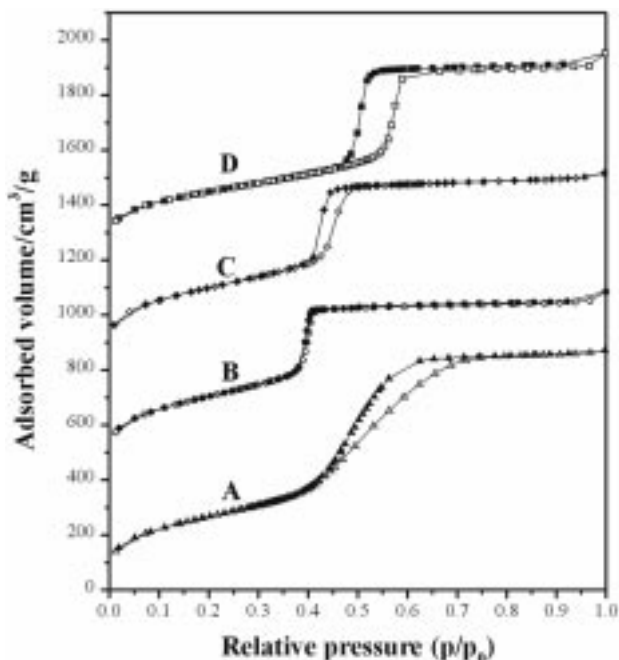


Fig. 2. N_2 adsorption-desorption isotherms of the $C_{18}TMACl-HNO_3-TEOS-H_2O$ mesoporous silica before and after ammonia hydrothermal treatment at different temperatures and reaction times. A) before ammonia hydrothermal treatment. B) hydrothermal treatment at $100^\circ C$ for 4 days. C) hydrothermal treatment at $150^\circ C$ for 1 day. D) hydrothermal treatment at $150^\circ C$ for 2 days.

Let us now focus on the rope morphology. The exterior looks of the ropes (Fig. 3A) are bundles of fibers as reported previously, and this is preserved after ammonia hydrothermal treatment;^[4] in contrast, however, the ends of the ropes change. We took scanning electron microscopy (SEM) micrographs of broken ends of the fiber before (Fig. 3A) and after hydrothermal treatment (Fig. 3B). Before hydrothermal treatment, the broken ends look smooth and nothing unusual. But after hydrothermal reaction, one sees extraordinary myelin figures grown from the ends. Their diameters and length are 80–150 nm and 300–400 nm respectively. The transmission electron microscopy (TEM) magnification of these nano-sized silica tubules is shown in Fig. 3C. It looks rather like multi-walled carbon nanotubes. The TEM shows hexagonal channels in the nano-tubules, which run parallel to the axis. At the head of the tubule exists a defect of $+\pi$ disclination. The single $+\pi$ disclination is seldom observed in mesoporous silica materials.^[9,10] As far as we are aware these are the smallest tubules observed in mesoporous silica. Now both the myelin's appearance and its circumstance are very much similar to those "myelin figures" observed in phospholipid bilayers,^[11] although diameter of the latter is usually bigger, in the micron range. Recently, it has been observed that myelins can also be grown from an AOT/brine (AOT = sodium bis(2-ethylhexyl)sulfosuccinate) system.^[12] Although, there is yet no complete understanding of the myelin formation process, we do know that the myelin textures of water-lipid appears as a consequence of the swell-

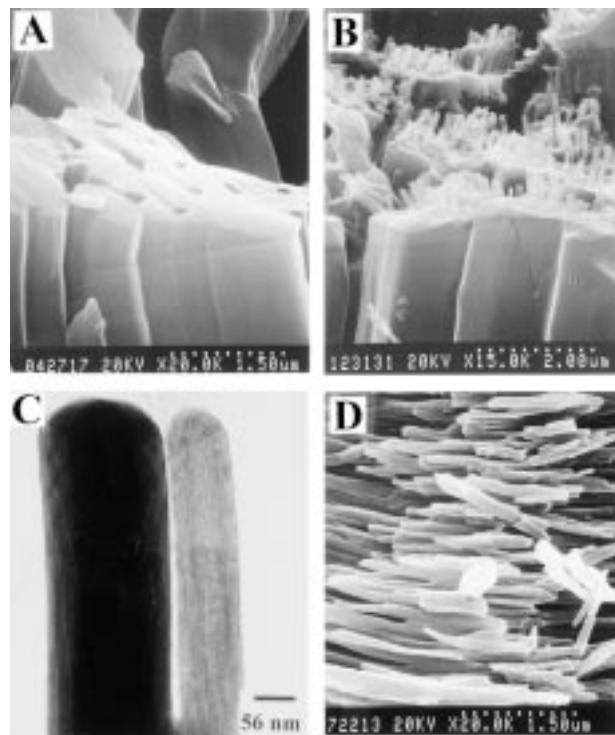


Fig. 3. The SEM and TEM micrographs with different magnification of the calcined silica ropes. A) Silica ropes before hydrothermal treatment. B) silica ropes after slight hydrothermal treatment. C) TEM micrograph of the silica tubes; D) silica nanotube bundles.

ing by increasing water content and dissolution of the bulk lamellar phase. This seems to be the situation in our observation of Figure 3B after ammonia-hydrothermal treatment at $150^\circ C$. The original "soft" as-synthesized product is supposed to be swollen (d_{100} from 3.8 nm to 5.2 nm, and pore size from 3.2 nm to 4.6 nm) by water in the ammonia solution at high temperature. At the same time, some surfactants are dissolved in the water. The pore expansion process would induce some surfactant (and associated silicates) backflow. If the swollen surfactant phase cannot intermediately dissolve into solution by molecular diffusion, this backflow brings about the formation of myelin figures. In contrast, the myelin figures cannot be formed in $100^\circ C$ hydrothermal conditions, where pore expansion was not observed. Thus, the structural swelling should be the determining factor for the formation of the myelin figures of both lamellar water-lipid and hexagonal surfactant-silica systems.

After extensive hydrothermal treatment, some silica fibers would become deeply etched to form bundles of silica nanotubes as shown in the SEM micrographs in Figure 3D. The nanotubes are parallel and have uniform diameter (about 100 nm). Previously, many researchers have observed tubular forms of mesoporous silica. But they are always above a micrometer in diameter. This is the first time the tubular form of mesoporous silica has been obtained in the nanometer range.

Let us further take the myelin dissolution explanation to see if it can also explain the drastic changes in gyroids after

hydrothermal treatment. One should note that the partial dissolution of surfactants occurs only for the acid synthesis route because of its weaker interaction in $S^+X^-T^+$, instead of the strong interaction S^-T^+ operating in the alkaline route.^[4,13]

For the production of gyroidal spheres, we used $C_{16}TAB$ as the template in the acid route. The interior of the as-synthesized gyroids is filled with silica-surfactant materials. After ammonia hydrothermal treatment at 150 °C for 2 days, the SEM micrograph shows that many of the gyroidal spheres are broken, revealing the interior as hollow with a center pillar (Fig. 4A). The outer appearance seems to be the same as the as-synthesized samples. Under higher magnification, one finds the shells of the hollow gyroidal spheres to be very thin—less than 0.2 μm —and the outer texture of the gyroid was preserved (Fig. 4B). Given the thin shell, the hollow gyroidal sphere is fragile and easily broken. The pillar-within-gyroids structure is in striking resemblance to our previously reported hollow pillar-within-sphere (PWS) that was synthesized from alkaline solution of $C_{14}TMAB$ -BuOH-silicate- H_2O system.^[11] The resemblance of outer look is not superficial. They have a similar underlying structure. Both spheres are supported by a center pillar with nanochannels running in the latitude direction.

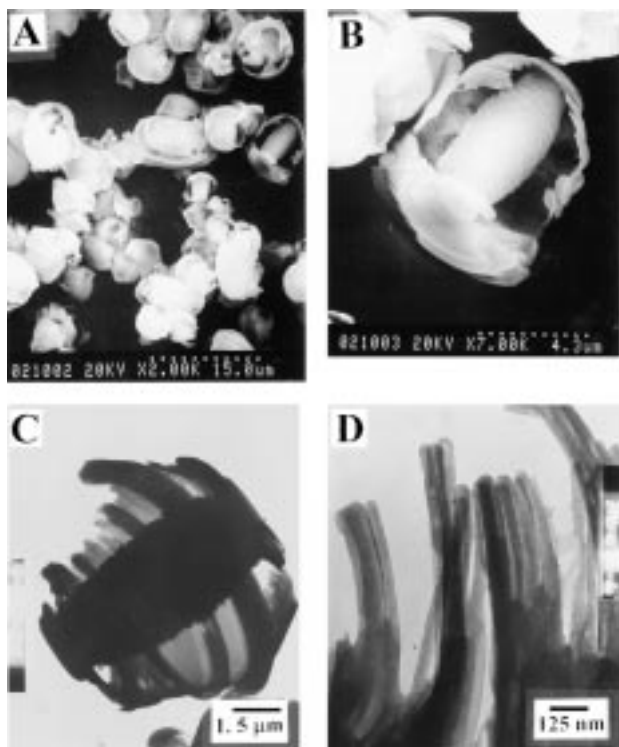


Fig. 4. The SEM and TEM micrographs with different magnification of the hollow gyroidal. A) SEM of hollow gyroids; B) SEM of the pillar-within-gyroid; C) TEM of a hollow gyroidal; D) TEM of the broken shell of the hollow gyroid.

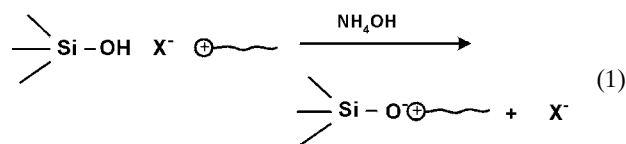
During the hydrothermal process at higher temperature, the nano-channels of less condensed silica species and sur-

factant in the interior of gyroidal spheres re-arrange. The nano-channels wind along the latitude direction as in the PWS reported by us.^[14] As in our previous PWS structure, when the circled nano-channels grow closer to the pole regions the energy for bending the channels increases with the curvature. To minimize the bending energy, the inner pillars are formed at the center of the gyroidal spheres.

The outer surface of gyroids seems to be preserved after hydrothermal treatment. This indicates that silicon–oxygen bond condensation is rather complete at the outer shell; so they are far less susceptible to alkaline attack. On the other hand, there must be some surfactant dissolution, which must happen inside the gyroids. Again, the myelin dissolution mechanism seems to work here. Figure 4C shows a TEM micrograph of a broken hollow gyroid. Several interesting appearances can be noted here. Although all the mesoporous channels on the shell appear to run along the latitude direction, they are not uniformly bundled. There are two different regimes on the shell. The darker “rings” appear to correspond to the steps on the outer surface while the less dense shell consists of disconnected individual tubules running in latitude direction. The darker part is the place where crystallization is more complete and more stable towards alkaline attack. Here, the parallel tubules are denser. Figure 4D shows that the parallel nano-tubes of the mesoporous silica are formed on the broken thin shell. Their diameters are about 50 nm and there also exists a $+\pi$ disclination. Thus, the myelin figures can also be formed on the thin shell.

One question that concerns us is how these nano-sized tubules are formed on gyroidal spheres in the hydrothermal stage. If we take the myelin hypothesis, the shell can be taken as the residue silica after the dissolution of the myelin. It seems that the myelin departure takes place inside the gyroids; one can see the inner surfaces of the gyroids are rough consisting of many loose nano-tubes (Fig. 4B). So after extensively dissolving the surfactants in hydrothermal treatment, there is empty space inside the gyroid sphere. Finally, the undissolved nano-tubes stick to the inner pillar to create the loose structure of the pillar.

Another important question is the role of ammonium hydroxide in hydrothermal treatment. By treating the as-synthesized materials from acid route with ammonia solution, the interaction between the surfactant and silicate would be transformed from the weaker $S^+X^-T^+$ electrostatic interaction to the stronger S^-T^+ interaction:



where $X^- = \text{NO}_3^-, \text{Br}^-, \text{Cl}^-, \text{SO}_4^{2-}$.

Under hydrothermal treatment at high temperature, the less-condensed silica species and the surfactant molecule would subsequently re-arrange by the myelin dissolution

process to form nanotubes of mesoporous silica. More remains to be learned about the role of ammonia in the hydrothermal treatment. Recently, Stucky and coworkers employed small amounts of NH_4F in an acid synthesis with block copolymer templates.^[15] They obtained bundles of silica fibers similar in outer appearance to our bundles of silica nanotubes.^[16] It is not clear what mechanism is operating in their acid synthesis.

In conclusion, the millimeter-sized silica ropes and hollow gyroidal spheres with well-aligned hexagonal mesostructure of expanded pores have been synthesized in a novel two-step procedure. Besides the hierarchical structures, the nano-scaled mesoporous tubules and myelin fingers are formed at the broken end of the fibers and the shell of hollow gyroids. Although the formation mechanism of these fascinating structures is still not completely understood, we believe that this novel two-step procedure is significant not only for understanding the morphology change of silica but also for producing special hierarchical structures of the mesoporous materials for various applications.

Experimental

Synthesis: Mesoporous silica was prepared in a convenient two-step procedure. In the first step, the templating agent $\text{C}_{18}\text{TMACl}$ (Tokyo Chemical Industry) or C_{16}TMAb (Acrôs) was dissolved in water, then the nitric acid was added (Acrôs) to give a highly-viscous and clear solution. To this solution, the silica source tetraethyl orthosilicate (TEOS, Acrôs) was added under stirring at 40 °C or 32 °C. The gel composition is (in moles) 1 surfactant: (3.0–15.0) TEOS : (5.0–40.0) HNO_3 : (1000–3000) H_2O . The gel solution was then allowed to stir for 5 to 10 h. The products were filtered and washed with deionized water and dried at 100 °C. Second, 1.0 g of dried sample was added to 50.0 g of 1.0 M NH_4OH aqueous solution and sealed in an autoclave, then put into an oven at 100, 130, or 150 °C for 4 days. The final resultant was collected by filtration, washed, and dried at 100 °C. The organic structure-directing agents were removed by calcination at 560 °C for 6 h in air.

Characterization: X-ray powder diffraction (XRD) data were collected on a Scintag X1 diffractometer using $\text{Cu K}\alpha$ radiation ($\lambda = 0.154$ nm). The N_2 adsorption–desorption isotherms were obtained at 77 K on a Micrometric ASAP 2100 apparatus. The SEM was taken on a S-800 (Hitachi) operated at an accelerating voltage of 20 keV. The ultra-thin TEMs were made on a Hitachi H-7100 operated at 100 keV.

Received: August 5, 1999

Final version: November 5, 1999

- [1] C. T. Kresge, M. E. Leonowicz, W. J. Roth, J. C. Vartuli, J. S. Beck, *Nature* **1992**, 359, 710.
- [2] J. S. Beck, J. C. Vartuli, W. J. Roth, M. E. Leonowicz, C. T. Kresge, K. D. Schmitt, C. T.-W. Chu, D. H. Olson, E. W. Sheppard, S. B. Higgins, J. L. Schlenker, *J. Am. Chem. Soc.* **1992**, 114, 10834.
- [3] Q. Hou, S. I. Margolese, U. Ciesla, P. Feng, D. E. Gier, P. Sieger, B. F. R. Leon, P. M. Petroff, F. Schuth, G. D. Stucky, *Nature* **1994**, 368, 317.
- [4] a) H. P. Lin, S. B. Liu, C. Y. Mou, C. Y. Tang, *Chem. Comm.* **1999**, 583. b) H. P. Lin, C. Y. Mou, unpublished.
- [5] H. Yang, N. Coombs, G. A., Ozin, *Nature* **1997**, 386, 692. b) G. A. Ozin, H. Yang, I. Sokolov, N. Coombs, *Adv. Mater.* **1997**, 9, 662.
- [6] D. Khushalani, A. Kuperman, G. A., Ozin, K. Tanaka, J. Garcés, M. M. Olken, N. Coombs, *Adv. Mater.* **1995**, 7, 842.
- [7] C. F. Cheng, W. Z. Zhou, J. Klinowski, *Chem. Phys. Lett.* **1996**, 263, 247. b) W. Z. Zhou, J. Klinowski, *Chem. Phys. Lett.* **1998**, 292, 207.
- [8] M. Kruk, M. Jaroniec, A. Sayari, *J. Phys. Chem. B* **1999**, 103, 4590.
- [9] J. Feng, Q. Huo, P. M. Petroff, G. D. Stucky, *Appl. Phys. Lett.* **1997**, 71, 1887.

- [10] a) I. Sokolov, H. Yang, G. A. Ozin, C. T. Kresge, *Adv. Mater.* **1999**, 11, 636. b) G. A. Ozin, H. Yang, N. Coombs, I. Sokolov, *J. Mater. Chem.* **1998**, 8, 743.
- [11] I. Sakurai, Y. Kawamura, *Biochim. Biophys. Acta* **1984**, 777, 347. b) I. Sakurai, T. Suzuki, S. Sakurai, *Biochim. Biophys. Acta* **1989**, 985, 101.
- [12] M. Buchanan, J. Arrault, M. E. Cates, *Langmuir* **1998**, 14, 7371.
- [13] Q. Hou, S. I. Margolese, U. Ciesla, D. G. Demuth, P. Feng, D. E. Gier, P. Sieger, B. F. Chmelka, F. Schüth, G. D. Stucky, *Chem. Mater.* **1994**, 6, 1176.
- [14] H. P. Lin, Y. R. Cheng, C. Y. Mou, *Chem. Mater.* **1998**, 10, 3772.
- [15] D. Zhao, J. Feng, Q. Huo, N. Melosh, G. H. Fredrickson, B. F. Chmelka, G. D. Stucky, *Science* **1998**, 279, 548.
- [16] P. Schmidt-Winkel, P. Yang, D. I. Margolese, B. F. Chmelka, G. D. Stucky, *Adv. Mater.* **1998**, 11, 303.

A Facile Nanoparticle Synthesis Within a Polar Polysulfone Active Matrix**

By Amir Weitz, Jack Worrall, and Fred Wudl*

Quantum confinement in semiconducting materials of nanometer dimensioned crystallites and its implications regarding physical, chemical, and optical properties have drawn much attention in recent years.^[1] Interpretation of any experimental observations that are truly inherent to the nanometer-size regime has to be related to the size and quality of the particles.^[2] Finding a facile organic synthetic route to these materials was, and still is, one of the main challenges^[2,3] but substantial progress has been reported in the last decade.^[4]

Extensive research has led to the development of many synthetic routes that yield monodisperse nanoparticles. One recent, and most common, method to generate monodisperse nanocrystallites is based on the pyrolysis of organometallic reagents by injection into a hot coordinating solvent.^[2] Using polymers in the synthesis of nanoparticles should yield a composite that has processable qualities, which other approaches do not provide. Excluding a few examples,^[4,5] in most of the work related to the synthesis of nanoparticles utilizing polymers; the polymer was merely used as a passivating matrix for encapsulating the particles formed by titration methods with inorganic salts^[6] or as a sophisticated phase-segregating matrix of block copolymers.^[4a-c,e] Using a functional group within a polymer to generate monodisperse particles via a reaction with inorganic nanoparticle precursor should yield particles that are embedded in a passivating organic matrix as they are formed. This approach would be very versatile and general; e.g., different inorganic precursors can be used in their reaction with different functional groups. Reactions that can be carried out with inorganic solids and not salts; e.g., metal

[*] Prof. F. Wudl, Dr. A. Weitz
Department of Chemistry and Biochemistry
Exotic Materials Institute, University of California
Los Angeles, CA 90095-1569 (USA)

Dr. J. Worrall
Director of operations at CEMMA University of Southern California
Los Angeles, CA 90089 (USA)

[**] We thank the Office of Naval Research for support through grant N000149710835.